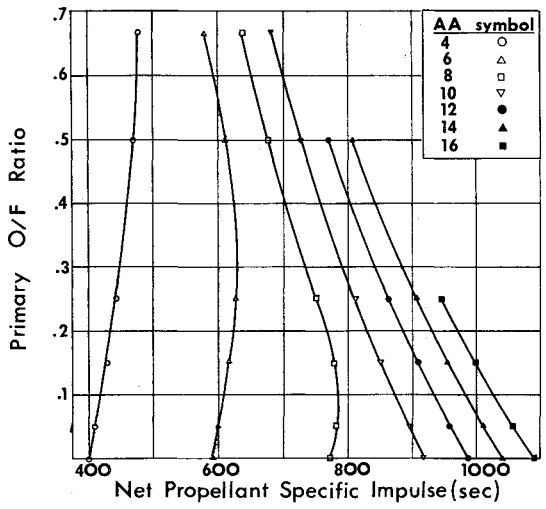

Fig. 4 Propellant I_s vs propellant composition.

the ram air, and this energy is added to the nitrogen and oxygen as heats of formation data. The specific impulse values, output by the computer program are then based on the mass flux of the total mixture, fuel, oxidizer, and air. The computer program output is then converted to net specific impulse based on the flow rate of the airborne propellant.

The specific impulse output by the computer program ($I_{s(M)}$) may also be called the mixture specific impulse output and is defined as

$$(I_{s(M)} = F_j/(\dot{w}_o + \dot{w}_f + \dot{w}_{\text{air}})$$

In this note, air augmentation ratio is defined as

$$AA = \dot{w}_{\text{air}}/(\dot{w}_o + \dot{w}_f)$$

Therefore, the specific impulse based on onboard propellant flow rate is

$$I_{s(p)} = (1 + AA)I_{s(M)}$$

A consideration of system energy shows that the net thrust of an air-augmented system may be equated as

$$F_n = (P_e A_e + \dot{w}_m V_e/g) - (P_e A_\infty + \dot{w}_{\text{air}} V_\infty/g) - P_e(A_e - A_\infty)$$

When the ramrocket's exhaust stream is optimally expanded to ambient pressure,

$$F_n = (\dot{w}_m V_e/g) - (\dot{w}_{\text{air}} V_\infty/g)$$

However,

$$F_j = \dot{w}_m V_e/g$$

$$I_{s(P,\,N)} = (1 + AA)I_{s(M)} - AA(V_\infty/g)$$

Several cases were calculated using RFNA/MAF-4 as the onboard propellant system. In the calculated cases the flight condition was Mach 1.5 at sea level. Figure 2 is a plot of mixture specific impulse values vs air augmentation ratios for several onboard propellant O/F ratios. Figure 3 is a presentation of net propellant specific impulse vs air augmentation ratios for the several onboard propellant O/F ratios. Figure 4 presents the same information as Fig. 3 but with a different emphasis.

Discussion

Presently available chemical equilibrium compositions computer programs can be used for the calculation of ramrocket and ramjet propellant performance data. The chemical equilibrium composition programs usually concern themselves only with the combustion products flow as it enters and passes through a supersonic nozzle. The method developed in this note permits calculation of maximum net specific impulse values through treatment of the ram air as a portion of the oxidizer system and by considering that the combustion products are homogeneous mixtures during ideal supersonic expansions.

Figure 2 notes that the mixture specific impulse curves understandably shift toward higher air augmentation ratios as the airborne propellant system becomes increasingly fuel-rich.

Figure 3 presents net specific impulse vs air augmentation ratios, and here the performance curves demonstrate crossovers as air augmentation increases. At low air augmentation ratios the onboard propellant streams with the highest O/F ratios possess the larger specific impulses. As the air augmentation ratios are increased, those onboard propellant streams with the smallest O/F ratios have greater thrust capability.

Figure 4 highlights the influence of the onboard propellant's O/F ratio on net specific impulse for given air augmentation ratios. This mode of presentation is useful in making air augmentation tradeoff studies.

The method of calculation described in this paper applies equally well to ramjet propellant performance determinations. In a ramjet system, the onboard propellant consists only of fuel, and the onboard propellant O/F ratio for these cases is zero, resulting in a single curve for each fuel considered.

The examples used here featured a liquid onboard propellant system of red fuming nitric acid and a mixed amine fuel. Solid propellants can also be used as onboard propellants with the same chemical equilibrium compositions computer program.

In conclusion, the method described here greatly extends the utility of presently available chemical equilibrium compositions computer programs. These programs can now be employed to make ramrocket and ramjet propellant performance calculations in addition to their original rocket propellant performance uses.

Buckling of Circular Conical Shells under Uniform Axial Compression

JOSEF SINGER*
Technion, Israel Institute of Technology, Haifa, Israel

Nomenclature

a	=	distance of the top of a truncated cone from the vertex, along a generator
C_n	=	displacement coefficient of the nth term of w
E	=	modulus of elasticity
h	=	thickness of shell
H_2, H_2^{-1}	=	differential operators defined by Eqs. (6) and (48) of Ref. 3
K^4	=	$12\,(1 - \nu^2)(a/h)^2$
m, n	=	integers
P	=	axial force
P_{cyl}	=	axisymmetric buckling load of corresponding cylindrical shell
u, v, w	=	nondimensional displacements, obtained by dividing the physical displacements by a
x	=	nondimensional axial coordinate along a generator

Received December 7, 1964. The research reported in this note has been sponsored by the Air Force Office of Scientific Research (OAR) under Grant No. AF EOAR 63-58 with the European Office of Aerospace Research, U. S. Air Force. The author wishes to thank O. Harari and J. Stern for their help with the computations.

* Associate Professor, Department of Aeronautical Engineering. Member AIAA.

Table 1 Critical load for typical conical shells under uniform axial compression

Typical shell	α, deg	x_2	Taper ratio, $1 - x_2$	ν	ρ_{av}/h	$(P_{cr}/E) \times 10^3$ 1-term	2-term	3-term	4-term	5-term	7-term	$(P_{cr}/E) \times 10^3$, axisymmetric
a	30	1.5	0.333	0.30	831	28.76	28.53	28.33	28.25	...	...	28.52
b	40	5.0	0.80	0.33	488	0.6168	0.6017	0.5785	...	0.5654	0.5564	0.563

x_2 = ratio of the distance of the bottom of a truncated cone from the vertex to that of the top
α = cone angle
β = $(\pi/lg_e x_2)$
γ = $(1 - \nu)/2$

IN Ref. 1 the axisymmetrical buckling of conical shells under axial compression was investigated. By setting Poisson's ratio equal to zero (with the justification that buckling loads are usually not sensitive to Poisson's ratio), the buckling load was found to be

$$P_{cr} = P_{cyl} \cos^2\alpha = \{2\pi Eh^2/[3(1 - \nu^2)]^{1/2}\} \cos^2\alpha \quad (1)$$

In Ref. 2 the buckling under axial compression and external or internal uniform hydrostatic pressure was analyzed without prescribing axisymmetry. For the case of axial compression and internal pressure the axisymmetrical buckling mode predominates, whereas for axial compression and external pressure the more general mode with many lobes along the circumference is critical. Buckling loads for axial compression only were not computed in this analysis because of the very poor convergence of the stability determinant for zero external (or internal) pressure. For this case, the approximation of Eq. (1) was assumed to hold, since some spot calculations indicated it to be sufficiently accurate. Both Refs. 1 and 2 assume simple supports defined by the geometric (essential) boundary conditions

$$w \cos\alpha - u \sin\alpha = 0 \qquad v = 0 \text{ at } x = 1, x_2 \quad (2)$$

representing bulkheads that are rigid in a plane perpendicular to the axis and very flexible in the axial direction; whereas in this note the usual simple-support conditions for conical shells are assumed which are defined (as for cylindrical shells) by the geometric boundary conditions

$$w = 0 \qquad v = 0 \text{ at } x = 1, x_2 \quad (3)$$

and represent bulkheads that are rigid in the radial direction and very flexible in the direction of the generators. (Both definitions imply the natural boundary conditions of free rotation of generators about the edges and freedom from restraint in the direction of the axis or the generators, respectively.)

The method of Ref. 3 (which is also a linear theory) is therefore extended and applied to the analysis of buckling under uniform axial compression. This method of solution implies elastic restraints that approximate the condition of $v = 0$ very closely; the effect of the u restraint has been found to be practically negligible in the cases of external pressure and torsion. In Ref. 4, the effect of axial constraint on the instability of circular cylindrical shells under uniform axial compression was shown to be even smaller than in the case of external pressure loading, and hence its effect can also be neglected here.

The membrane stresses in the case of uniform axial compression are

$$\left.\begin{aligned} \bar{\sigma}_x &= -(P/2\pi hax \sin\alpha \cos\alpha) \\ \bar{\sigma}_\phi &= 0 \qquad \bar{\tau}_{x\phi} = 0 \end{aligned}\right\} \quad (4)$$

Now, assuming that for the buckling analysis the prebuckling stress is represented satisfactorily by the membrane stresses [Eq. (4)], the modified third stability equation [Eq. (49) of Ref. 3] becomes

$$(1/x^2 \sin^2\alpha)H_2(w) + K^4(P/E)(1/2\pi hax \sin\alpha \cos\alpha)w_{,xx} + (1/x^3)K^4 \cos^2\alpha H_2^{-1}[(x^3 w_{,xx})_{,xx}] = 0 \quad (5)$$

Substitution of the solution of Ref. 3 in Eq. (5), and evaluation by the Galerkin method, yields after some manipulations

$$\Sigma C_n\{[(-1)^{m+n}x_2^{2\gamma-2} - 1]G_1(n,m) + K^4 \cos^2\alpha[(-1)^{m+n}x_2^{2\gamma} - 1]G_2(n,m) + \eta[(-1)^{m+n}x_2^{2\gamma-1} - 1]G_5(n,m)\} = 0 \quad [6]$$

where $G_1(n,m)$ and $G_2(n,m)$ are algebraic expressions given by Eqs. (64–66) of Ref. 3

$$G_5(n,m) = K_3(n)\left[\frac{m+n}{(2\gamma-1)^2 + (m+n)^2\beta^2} + \frac{m-n}{(2\gamma-1)^2 + (m-n)^2\beta^2}\right] + K_4(n) \times \left[\frac{1}{(2\gamma-1)^2 + (m+n)^2\beta^2} - \frac{1}{(2\gamma-1)^2 + (m-n)^2\beta^2}\right] \quad (7)$$

$$K_3(n) = n\beta^2(2\gamma - 1) \quad (8)$$

$$K_4(n) = (2\gamma - 1)[(\gamma^2 - \gamma) - n^2\beta^2] \quad (9)$$

$$\eta = (P/E)(K^4/2\pi h\alpha \sin\alpha \cos\alpha) \quad (10)$$

N linear equations are obtained for an N-term solution, and the lowest eigenvalue η of the determinant of the coefficients of C_n yields the buckling load. However, it should be noted that, whereas in the case of buckling under external pressure[3] $n = 1$ is always the basic mode (which consists of one half-wave in the axial direction), here the value of n of the basic mode is determined by the geometry of the shell and is usually larger than unity.

Hence the summation in Eq. (6) for an N-term solution, should not extend from $n = 1$ to N, but from $n = n_b$ to $(N - n_b + 1)$, where n_b is the number of half-waves in the axial direction of the basic mode (n_b may, however, sometimes be unity). It should be remembered that, as in the case of external pressure, the integral value of t (the number of circumferential waves) which yields the minimum buckling load must be used in the calculations.

The critical loads were calculated for two typical shells, one short shell and one long one, by one-, two-, three-, four-, five-, and seven-term solutions and compared with the approximate axisymmetric solution of Eq. (1). The results are tabulated in Table 1. As in Ref. 1, the convergence is much slower for a shell of large taper ratio, shell b. The asymmetrical buckling loads are found to be very slightly below the axisymmetric ones in these examples.

The instability behavior of thin conical shells, under axial compression, within the bounds of linear theory, is hence similar to that of cylindrical shells. The disagreement of the predictions of linear theory with experimental results is also similar,[5–7] but the linear analysis has practical value in cases of combined loading and for orthotropic or closely stiffened shells.

References

[1] Seide, P., "Axisymmetrical buckling of circular cones under axial compression," J. Appl. Mech. **23**, 625–628 (1956).

[2] Seide, P., "The stability of thin conical frustrums subjected to axial compression and internal or external uniform hydrostatic pressure," Space Technology Labs. Inc., Rept. AF BMD-TR-61-37 (March 1961).

[3] Singer, J., "Buckling of conical shells under axisymmetrical external pressure," J. Mech. Eng. Sci., **3**, 330–339 (1961).

[4] Singer, J., "The effect of axial constraint on the instability of thin circular cylindrical shells under uniform axial compression," Intern. J. Mech. Sci. **4**, 253–258 (1962).

[5] Lackman, L. and Penzien, J., "Buckling of circular cones under axial compression," J. Appl. Mech. **27**, 458–460 (1960).

[6] Weingarten, V. I., Morgan, E. J., and Seide, P., "Final report on the development of design criteria for elastic stability of thin shell structures," Space Technology Labs., Los Angeles, TR-60-0000-19425 (December 1960).

[7] Schnell, W. and Schiffner, K., "Experimentelle Untersuchungen des Stabilitätsverhaltens von dünnwandigen Kegelschalen unter Axiallast und Innendruck," Deut. Vers. Luft Raumfahrt, DVL Rept. 243 (November 1962).

Supersonic and Hypersonic Flow of an Ideal Gas around an Elliptic Nose

R. Douglas Archer*
University of New South Wales, Kensington, New South Wales, Australia
AND
Rudolf Hermann†
University of Alabama, Huntsville, Ala.

THE direct method of Dorodnitsyn[1] and Belotserkovskii[2–4] has been applied to obtain a first-order (one-strip) solution to the inviscid equations of the mixed subsonic-supersonic flow of a perfect gas about the nose of an elliptic cylinder. The equations were written[5] in coordinates along and normal to the body surface, as first used by Traugott[6] (see Fig. 1). This system enables bodies of arbitrary convex shape to be considered. In addition, by writing the equations in terms of the inverse of Mach number, an explicit solution was obtained for infinite Mach number. Thus the dimensionless freestream velocity becomes, using Traugott's notation,[6]

$$v_\infty^2 = \frac{1}{1 + 1/[(\gamma - 1)/2]M^2_\infty}$$

and the components of the velocity at the shock wave are

$$v_{s\delta} = v_\infty[\cos\theta - (1 - \epsilon)\cos\chi\cos(\theta + \chi)]$$

$$v_{n\delta} = v_\infty[-\sin\theta + (1 - \epsilon)\cos\chi\sin(\theta + \chi)]$$

Table 1 Stagnation-point shock standoff distance, first-order, one-strip Dorodnitsyn-Belotserkovskii (D-B) theory

	M_∞			
a/b	3.0	6.8	30	∞
0.5	0.4711	0.3166	...	0.2790
1.0	0.7016	0.4238	...	0.3728
2.0	0.8489	0.4946	...	0.4319
5.0	0.9306	0.5282	0.4599	0.4564
10.0	0.9446	0.5335	...	0.4604

Received December 21, 1964.

* Senior Lecturer, Mechanical Engineering School. Member AIAA.

† Director, Research Institute. Associate Fellow Member AIAA.

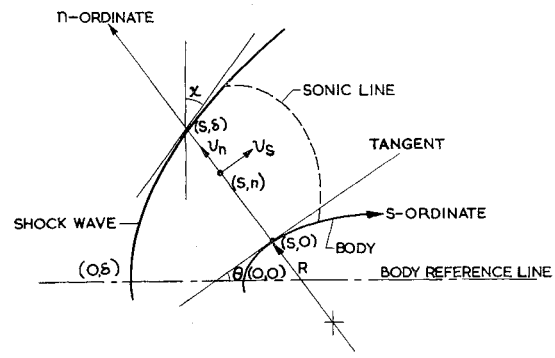

Fig. 1 δ-n coordinate system, Traugott.[6]

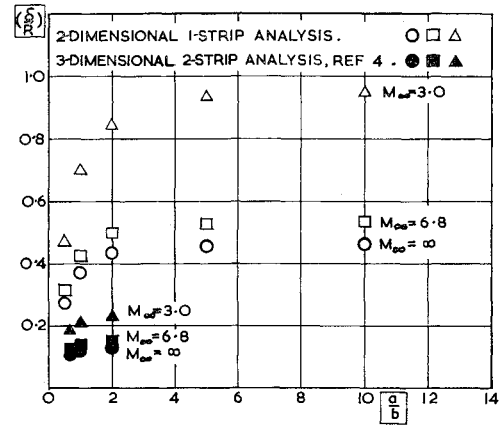

Fig. 2 Stagnation-point shock standoff distance, Dorodnitsyn-Belotserkovskii (D-B) method.

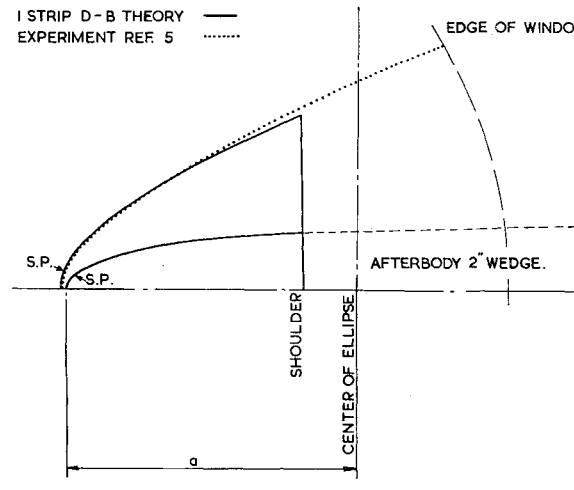

Fig. 3 Comparison of theoretical and experimental shock shape on elliptic cylinder, $a/b = 5$, $a = 3.046$ in., $R_0 = 0.122$ in., $M_\infty = 6.8$, $RN_\infty = 6.72 \times 10^4$/in.

where

$$\epsilon = [(\gamma - 1)/(\gamma + 1)](1 + w) = \rho_\infty/\rho_\delta$$

$$w = \frac{1}{[(\gamma - 1)/2]M_\infty^2\cos^2\chi}$$

The numerical analysis was performed on the Control Data Corporation 1604 at the University of Minnesota. Extrapolation to pass through the sonic singularity was made from 95 to 105% of sonic velocity and used a second-degree curve fit. Numerical integration was performed using the Adams-Moulton routine[7] with fixed step, the size of which was found to give